Nuclear Mathematical and Computational Sciences: A Century in Review, A Century Anew
Gatlinburg, Tennessee, April 6-11, 2003, on CD-ROM, American Nuclear Society, LaGrange Park, IL (2003)

The RTS&T Code as a Tool for Benchmarking of Evaluated Nuclear Data Files

I.I. Degtyarev, **O.A. Liashenko**, **and I.A. Yazynin**,
Institute for High Energy Physics,
142284, Protvino, Russia
degtyarev@mx.ihep.su; liashol@mail.ru; yazynin@mx.ihep.su

A.I. Blokhin,
Institute of Physics and Power Engineering, 249020 Obninsk, Russia
blokhin@ippe.obninsk.ru

V.I. Belyakov-Bodin,
Institute of Theoretical and Experimental Physics, 117259 Moscow, Russia
belyakov_b@vitep1.itep.ru

ABSTRACT

The paper describes the current status of general-purpose Monte Carlo code RTS&T [1]. New developments in modelling of discrete hadronic interactions (implementation of improved version for cascade-exciton model and modern nuclear data libraries) and results of computational studies of high power spallation thick ADS (Accelerator-Driven System) targets with 0.8-1.2 GeV proton beams are given. Comparison of experiments and calculations of double differential and integrated n/p yield is described also.

Key Words: particle production models, Monte Carlo simulation

1. INTRODUCTION

RTS&T (Radiation Transport Simulation and isotopes Transmutation calculation) is a general purpose Monte Carlo code system was assigned for detailed simulation of many particle types transport in a complex 3D geometry's with composite materials and calculation of particles fluences and functionals of radiation fields and isotopes transmutation problem as well.

A direct using of evaluated nuclear data files (ENDF/B-VI, JENDL, FENDL, BROND etc.) to simulate of radiation transport and isotopes transmutation problem in low- and intermediate-energy regions is a general idea of the RTS&T code.

Code can be successfully used to verify of continuous-energy data libraries were recorded in the ENDF format. It is possible to use the RTS&T code to criticality calculation and nuclear safety analysis. The main changes compared to the previous code version concern the hadron- and photo-production model in the intermediate and high energy regions, hadronic, photoatomic and photonuclear cross section compilations, improved data for charged particle energy losses in composite materials, and nuclear structure data (Fig. 1).

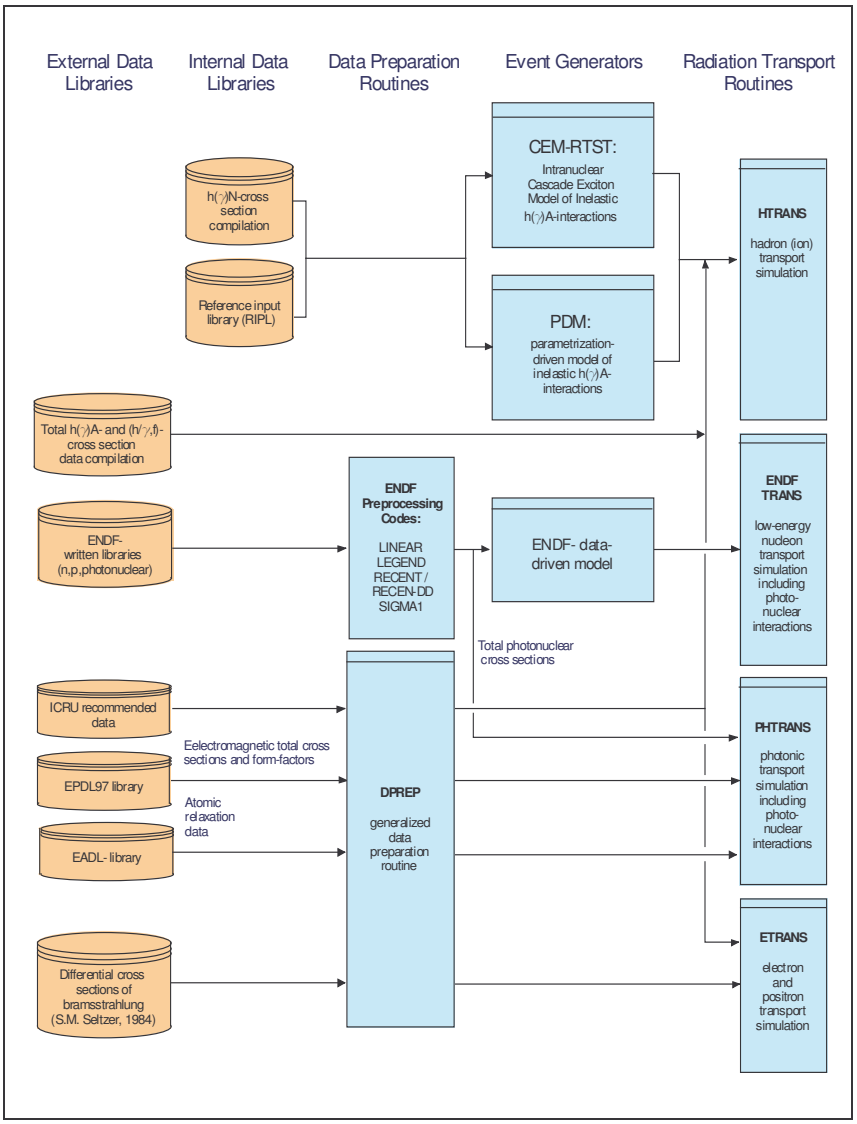

Figure 1. Flow chart of the data libraries used in the RTS&T code.

2. STANDARD PARTICLE PRODUCTION MODELS

Inelastic hadronic and photonic interactions are simulated within RTS&T code by several energy-dependent models based on the different microscopic and macroscopic approaches (Fig. 2).

2.1. Theory driven model (CEM-RTS&T)

The intra-nuclear cascade-exciton model is one of the most popular to simulate of the secondary particle parameters for the h(γ)A-inelastic scattering in the intermediate energy region. It allows one to reproduce the experimental observations up to energies about 0.1 to several-tens GeV. We have developed a new model version (CEM-RTS&T) and included it as event generator to the RTS&T code. In the CEM-RTS&T model the $h(\gamma)$ -induced nuclear reaction is assumed to be three-step process: intra-nuclear cascade (INC), pre-equilibrium emissions and decay of the equilibrated system (evaporation / binary fission processes competition). In the INC model nuclear structure is treated as a two-component degenerated Fermi-gas of nucleons in the spherical type of nuclear density.

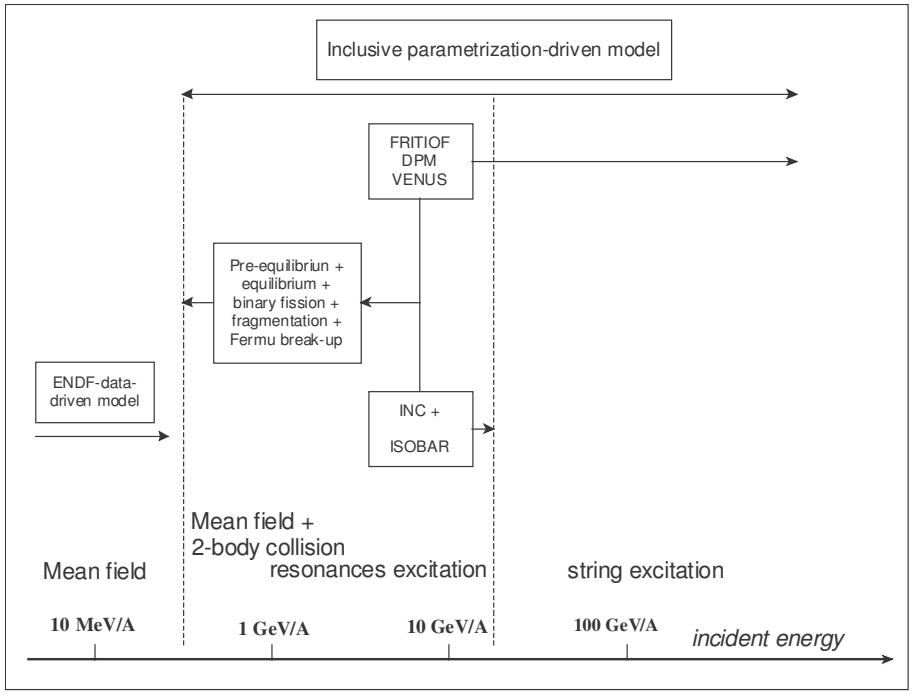

Figure 2. Particle production models implemented in the RTS&T code.

The phenomenological potential for nucleons is described as sum of the nuclear and Coulomb terms: $V^N(r) = V_N^N(r) + V_C(r)$, here $V_N^N(r) = T^F(r) + B(A,Z)$, where Fermi-energy depends on the local density of the nucleus $\rho(r)$, $T^F(r) = \frac{\hbar}{2m}\left[3\pi^2\rho(r)\right]^{1/3}$, $B(A,Z)$ is the nucleon binding energy. The nucleon distribution density is one of fundamental parameter for the INC model. The most popular Woods-Saxon form does not satisfy the two physical requirements, namely, the asymptotic behavior and the behavior near the center of the nucleus. The semi-phenomenological nucleon density distribution proposed by Gambhir and Patil [1] in the form:

$$\rho_i(r) = \rho_{oi}^N \left\{ 1 + \left[\frac{1}{2} + \frac{1}{2}\left(\frac{r}{R} \right)^2 \right]^{\alpha_i} \left[e^{\frac{r-R}{a_i}} + e^{-\frac{r+R}{a_i}} \right] \right\}^{-1} ,$$

where R is a measured size of nucleus and a_i and α_i are given in terms of the separation energy S_i of the last nucleon through: $a_i = \frac{\hbar}{2\sqrt{2mS_i}}$; $\alpha_i = \frac{q}{\hbar}\sqrt{\frac{m}{2S_i}} + 1$. Here m is the nucleon rest mass, $q = 0$ $(i = n)$ and $q = Z - 1$ $(i = p)$. This algebraic form designed has been tested in detail by comparing with the experiment the form factors for the electron scattering. The form of the Coulomb potential (only for protons) used in CEM-RTS&T is $V_c(r) = (Ze^2 / 2R_c)[3 - (r / R_c)^2]$ $(r \le R_c)$ and $V_c(r) = Ze^2 / r\,(r > R_c)$, where R_C is the Coulomb radius. The $\pi(K)A$-interaction potential is taken as $V^{\pi(K)}(r) = -V_0^{\pi(K)}\Theta(r)$, where $V_0^{\pi} = 25$ MeV, $V_0^{K} = 30$ MeV, and $\Theta(r)$ are the values of pion and kaon potential well and unit step function, respectively. The center-mass correlations are taken into account as proposed in Ref. [3]. One-particle nuclear density $\tilde{\rho}(\vec{r})$ taken from the equation:

$$\rho(\vec{r}) = \int \left[\prod_{i=1}^{A} \tilde{\rho}(\vec{r}_i) \right] \delta\left(\sum_{i=1}^{A} \frac{\vec{r}_i}{A} \right) \prod_{i=2}^{A} d^3\vec{r}_i \quad .$$

Here, $\vec{r}_i$ are the coordinates of i-th nucleon. The Pauli blocking is incorporated in the cascade simulation procedure. The effects of particle refraction by nuclear potential and the decrease of nucleon density during intra-nuclear cascade (co-called trawling effect) are taken into account also. The integral hh and γh cross sections is taken from the Particle Data Group compilation. Assuming the charge symmetry the following cross sections are taken identical: $\sigma_{nn} = \sigma_{pp}$, $\sigma_{\pi^- p} = \sigma_{\pi^+ n}, \sigma_{\pi^- n} = \sigma_{\pi^+ p}$, $\sigma_{K^0 p} = \sigma_{K^+ n}$, $\sigma_{K^0 n} = \sigma_{K^+ p}$. The isobar production channels covered by the INC model are presented in Table 1. The strange channels like $\gamma p \to \Sigma K^+, \Lambda K^+, \Lambda K^0 \pi^+$ and non-strange pseudoscalar and vector meson photoproduction channels $\gamma N \to [\rho / \varpi / \eta] N$ are included also. For multi-particle final states we adopt the CERN library GENBOD (W515) routine. The pre-equilibrium stage of the reaction is simulation in the frame of exciton model. The initial exciton configuration for pre-equilibrium decay formed in cascade stage of the reaction or postulated in general input ($2p1h$ configuration for incoming particle or $1p0h$ for incoming photon). The equilibrium stage of reaction (evaporation/fission processes) is performed according to the Weisskopf-Ewing statistical theory of particle emission and Bohr and Wheeler theory of fission. Double-humped fission barrier parameters for Z > 90 taken from the data set obtained in Obninsk and recommended by IAEA Reference Input Parameter Library (RIPL). Experimental single-humped fission barrier heights are incorporated in the CEM-RTS&T as proposed in Ref. [4], or can be calculated according to any phenomenological or theoretical models: Barashenkov et al. phenomenological approach; Barashenkov and Gereghi semi-phenomenological approach; liquid drop model (LDM) with Myers and Swiatecki parameters; LDM with Pauli and Ledergerber parameters; Krappe and Nix single-Yukawa modified LDM;

Krappe, Nix and Sierk Yukawa-plus-exponential modified LDM; Yukawa-plus-exponential modified LDM.

Table I. Baryon Resonance Production Channels

Entrance channel	Exit channel
pp	$p\Delta^+, n\Delta^{++}, \Delta^+\Delta^+, \Delta^0\Delta^{++}$
pn	$n\Delta^+, p\Delta^0, \Delta^0\Delta^+, \Delta^-\Delta^{++}$
γp	$\Delta^{++}\pi^-, \Delta^{++}\pi^0, \Delta^0\pi^+$
γn	$\Delta^+\pi^-, \Delta^0\pi^0, \Delta^-\pi^+$

The ratio of neutron emission to fission widths is taken in form proposed by Kupriyanov et al.:

$$\frac{\Gamma_n}{\Gamma_f} = \frac{\tilde{\Gamma}_n}{\tilde{\Gamma}_f} e^{-\frac{\delta W_g^{N-1}}{\tilde{T}_n} e^{-\lambda U_n} + \frac{\delta W_f}{\tilde{T}_f} e^{-\lambda U_f}},$$

where $\tilde{\Gamma}_n / \tilde{\Gamma}_f$ is Vandenbosch and Huizenga form of Fermi-gas model (asymptotic value occurring at high energies), δW is the shell correction term, λ=0.05 MeV. The post-fission parameters of the fragments are taken from the systematics by Adeev (Z_i, A_i) and Zhao et al. (T_{kin}). The inverse reaction cross section is calculated in form $\sigma_{inv}(T) = \sigma_{geom} T_b(T)$ with $\sigma_{geom} = \pi[R + R_b + \lambda\!\!\!^{-}]^2$ where σ_{geom}, R, R_b, $\lambda\!\!\!^{-}$ and $T_b(T)$ are the geometric cross section, radii of the potential residual nucleus and particle, the non-relativistic reduced channel wavelength and the non-relativistic s-wave Coulomb barrier transmission probability, respectively. The s-wave transmission factor is given by expression $T_b(\rho,\eta) = [F_0(\rho,\eta)^2 + G_0(\rho,\eta)^2]^{-2}$, where F_0, G_0 are the non-relativistic zero-order regular and irregular Coulomb wave-functions of variables $\rho = \hbar^{-1}(R_1 + R_2)(2\mu T_{cms})^{1/2}$, $\eta = \hbar^{-1} Z_1 Z_2 e^2 (\mu / 2T_{cms})^{1/2}$, where Z_1, Z_2, R_1, R_2 are the charge and radii of two particles, respectively, μ is the reduced mass of the two particle system, T_{cms} is the kinetic energy in cms. In the current version of RTS&T code the Fermi breakup model for disintegrating of light nuclei has replaced the evaporation model for nuclei with a mass number between 2 to 16. The evaporation of fragments with a mass number A > 4 does not included in current version RTS&T. The RIPL recommended Audi and Wapstra experimental compilation of atomic masses and binding energies is used in the RTS&T model. The level density parameter derived from the RIPL-systematics for any level density models: Gilbert-Cameron, back-shifted Fermi-gas model, Ignatyuk form of Fermi-gas model, generalized superfluid model (GSM), microscopic GSM, shell depended model proposed by Kataria and Ramamurthy, Mughabghab and Dunford systematic determined from the neutron resonance data.

To estimate of the averaged squared matrix element two different models can be used: estimation in approximation of quasi-free scattering of a nucleon above the Fermi level on a nucleon of the target nucleus [5] or by using a set of semi-empirical parametrizations. CEM-RTS&T has three different models to simulate the gamma-ray emission in pre-equilibrium and equilibrium stages: the Weisskopf single-particle model, the Brink-Axel GDR model, and the Kopecky-Uhl generalized Lorentzian model. To calculate the partial level densities for pre-equilibrium emission simulation the Avrigeanu systematic is used. Composite formulas include the advanced pairing and shell correction in addition to the Pauli blocking effect, and average energy-depended single-particle level densities for the excited particles and holes.

2.2. Parametrization-driven model (PDM)

The existing rigorous theoretical approaches and models allow estimate of various characteristics of secondary particle emission due to nuclear inelastic interactions, but they have uncertainly in choice of free parameters and the calculations are time-consuming. The RTS&T parametrization-driven model (PDM) is based on the modified systematics of double differential cross sections proposed in Refs. [6-9]. On the basis of the EXFOR experimental data library we obtained the improved parameters of Kalbach's systematics of parameters for quasi-free scattered nucleons and Sychev's systematic for cascade fraction of reaction. They represent a better statistical average, as they are based on more experimental data set. The RTS&T intra-nuclear-cascade-exciton model is employed to calculate the cross sections which not measured. For the spallation reaction, the PDM model is applied in a form of summation of the double differential cross sections for secondary particle emission expressed in the lab. frame by

$$\left(\frac{d^2\sigma}{dTd\Omega}\right)_{ij} = \sum_{k=1}^{7}\left(\frac{d^2\sigma}{dTd\Omega}\right)_k,$$

where i,j are the indexes of incident (γ, N,d,$\pi^{\pm}$, $K^{\pm}$, K^0, $\overline{N}$, ions) and secondary (γ, N, $\pi^{\pm}$, $K^{\pm}$, K^0, $\overline{N}$, ions, Δ, ρ, ω) particles. Components of k=1 to 7 correspond to the quasi-free and charge-exchange scattering, lider particle emission, production of cascade particles, the pre-equilibrium emission and equilibrium nuclear relaxation, the fragmentation, the binary fission, and parametrized in functional form:

$$\left(\frac{d^2\sigma}{dTd\Omega}\right)_k = \sigma_{in} n_{ij} \frac{dN}{dT} f(T,\theta),$$

where $\sigma_{in}, n_{ij}, \frac{dN}{dT}, f(T,\theta)$ are inelastic cross section, average multiplicity of secondary particles of j-th type, energy spectrum of the secondary particle, and energy-angle correlation function, respectively. At incident energies above $\sqrt{s} = 5$ GeV in addition to the processes 1-7 PDM takes into account inelastic diffractive scattering and shower particle generation. Differential cross sections of shower particles used in the invariant form originally proposed in [10]:

$$\frac{d^3\sigma^{h_1A\to h_2X}}{dp^3} = R\frac{d^3\sigma^{h_1p\to h_2X}}{dp^3},$$

where $\frac{d^3\sigma^{h_1p\to h_2X}}{dp^3}$ is the semi-empirical parametrization of the invariant inclusive cross section for one-particle production in hp-interactions, $R \equiv R(h_1, h_2, A, p_0, p, x_F)$ is the A-dependence function.

Analytical representation of double differential cross sections is used to local estimation of the radiation field functionals due to non-analog radiation transport simulation.

2.3. ENDF-data-driven model of low-energy $h(\gamma)A$ -interactions and transport

RTS&T uses continuous-energy nuclear and atomic evaluated data files to simulate of radiation transport and discrete interactions of the particles in the energy range from thermal energy up to 150 MeV. In contrast with the MCNP the ENDF-data driven model of the RTS&T code has access evaluated data directly. A first model version was originally develoved in 1997 to simulate of low-energy (up to 20 MeV) neutron transport using the neutronic part of the ENDF/B-VI evaluated data library. In current model development all data types provided by ENDF-6 format are takes account due to coupled multy-particle radiation transport modelling. Universal data reading and preparation procedure allows to use various data library written in the ENDF-6 format (JENDL, FENDL, CENDL, JEF, BROND, LA150, ENDF-HE/VI, IAEA Photonuclear Data Library etc.). ENDF data pre-processing (linearization, restoration of the resolved resonances, temperature dependent Doppler broadening of the cross sections and checking and correcting of angular distributions and Legendre coefficients for negative values are produced automatically with the Cullen's ENDF pre-processing codes LINEAR, RECENT (RECEN-DD for Reich-Moore parameters of several isotopes of JENDL library only), SIGMA1 and LEGEND [6] rewritten in ANSI standard FORTRAN-90. ENDF-recommended interpolation laws are used to minimize the amount of data. For data storage in memory and their further use the dynamically allocatable tree of objects (Fig. 3) is organized. All types of reactions provided by ENDF-6 format are taken into account due to particle transport modelling: elastic scattering, radiative capture and production of one neutron in the exit channel, absorption with production of other type particles (with division on excited states of the residual nucleus), the fission with separate yields of prompt and delayed neutrons and residual nucleus simulation by MF=8 data, etc. The energies and angles of emitted particles are simulated according to the distributions from MF=4, 5, 6, 12, 13, 14 and 15 files. For example, the following representations of outgoing energy-angle distributions for secondary particle can be used: tabular energy distributions, angular distributions via equally-probable cosine bins, Kalbach-Mann systematics for continuum energy-angle distributions (44 ENDF law), discrete two-body scattering, N-body phase-space energy distributions.

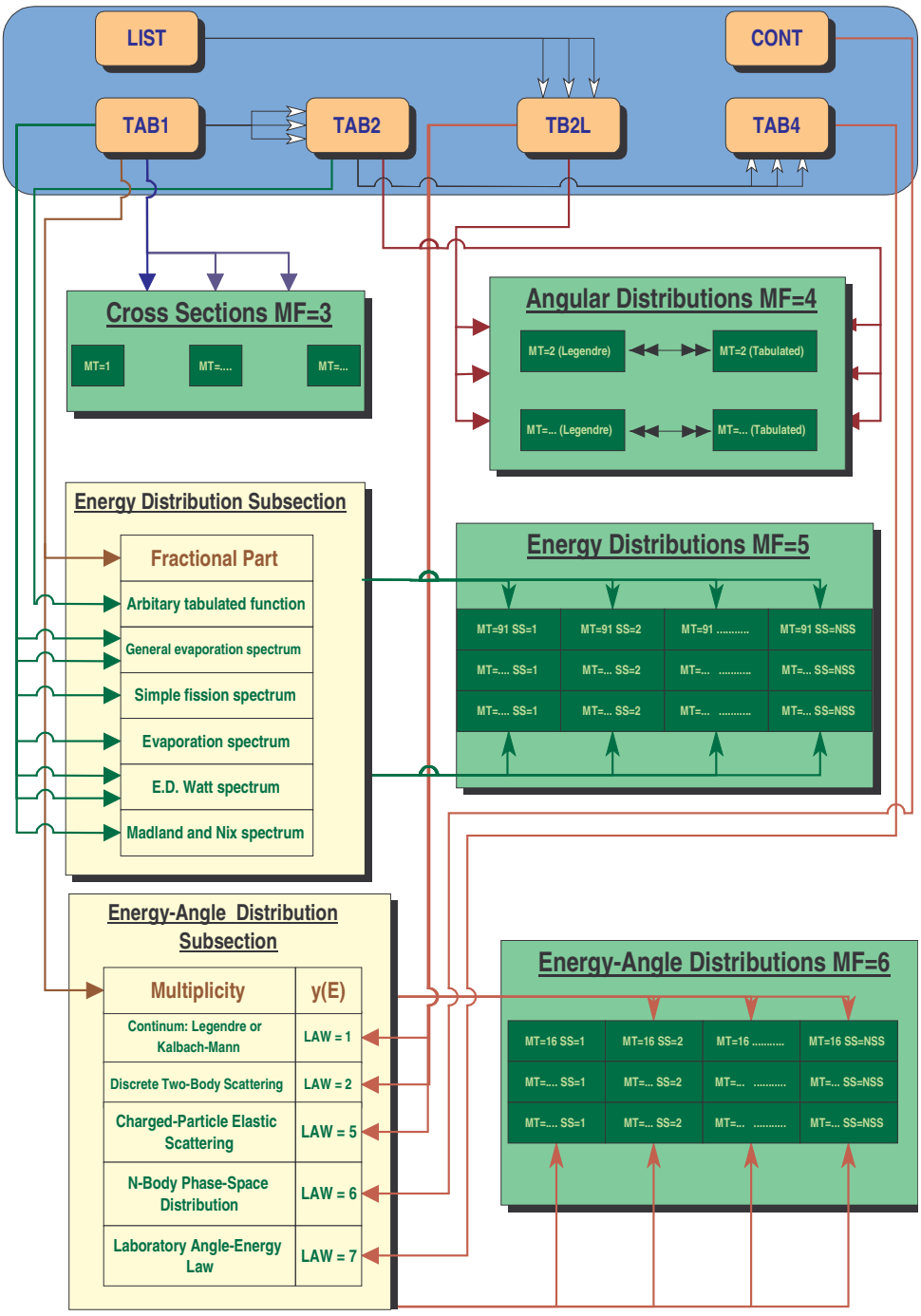

Figure 3. Block diagram of the ENDF data processing.

3. ALTERNATIVE AND ADDITIONAL PARTICLE PRODUCTION MODELS

As an alternative model to simulate of inelastic hA-interactions at intermediate and high energies, a three theory-driven generators may be used: DPMJET-II [11], FRITIOF (Version 7.02) [12] (modified as proposed in Ref. [13] to simulate of equilibrium particle emission, binary fission and nuclear fragmentation processes) and VENUS (Version 5.21) [14].

4. BENCHMARKING

For the validation of the PDM of the RTS&T code various test calculations were made for thin and thick targets in the energy region up to several GeV.

4.1. Thin target test calculations

A selective comparisons were made for the double differential cross section of secondary particles production in thin targets are presented in Figs. 4-6. Figs. 4,5 show the comparison with experimental data obtained from 1984 to 1990 in the LANL and the KFA and summarized in Ref. [15]. Fig. 6 show the comparison of the (p, Xn) double differential cross sections were obtained at angles varying from 0^o to 160^o with 1.2 GeV proton beam on a lead target at the SATURNE accelerator [16] with the calculated data by PDM. Comparison of the double differential neutron production cross sections in pion-initiated reaction at 870 MeV and 1 GeV are presented for lead in Fig. 10. The details of the experimental setup are reported in Refs. [17,18]. Solid lines stand for the calculated results of the PDM. Fig. 11 shows a total neutron multiplicity in (p, Xn)-reaction as a function of incident energy. Experimental data were derived from the Tesch's compilation.

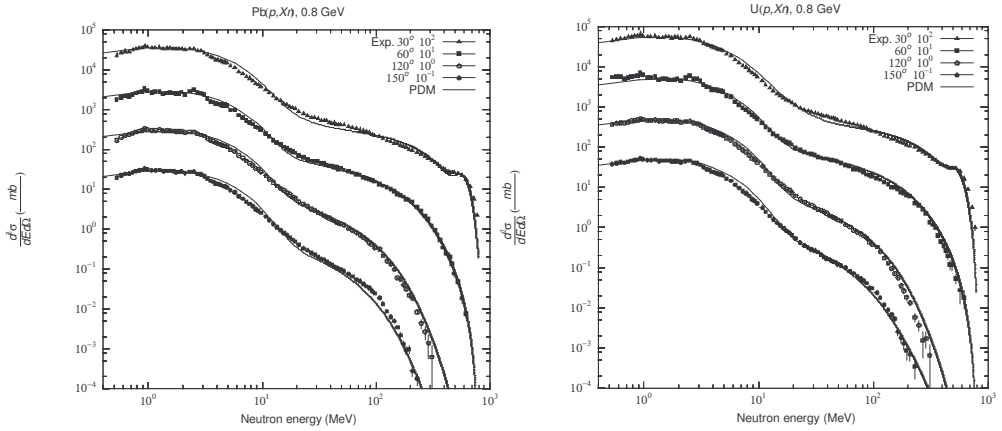

Figure 4. Comparison of neutron production cross section for Pb(p,Xn)-reaction at 0.8 GeV.

Figure 5. Comparison of neutron production cross section for U(p,Xn)-reaction at 0.8 GeV.

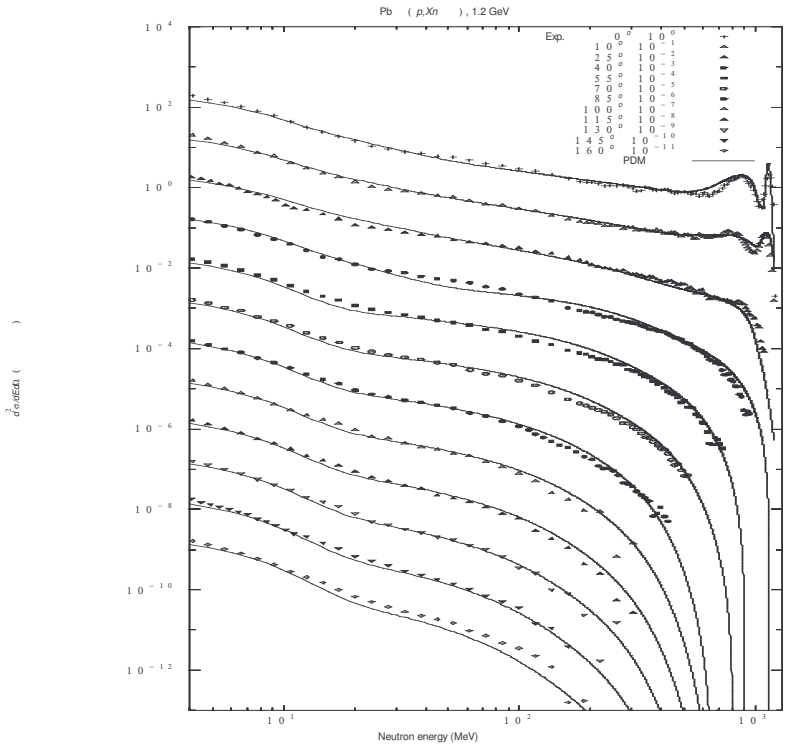

Figure 6. Comparison of neutron production cross section for Pb(p,Xn)-reaction at 1.2 GeV.

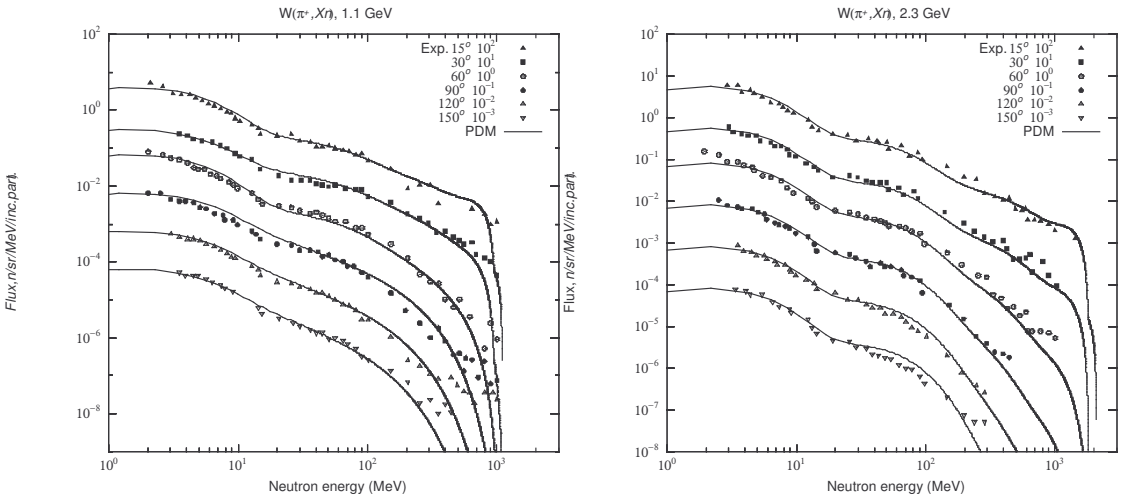

Figure 7. Comparison of neutron flux distribution from Pb(π^+,Xn)-reaction at 1.1 GeV.

Figure 8. Comparison of neutron flux distribution from Pb(π^+,Xn)-reaction at 2.3 GeV.

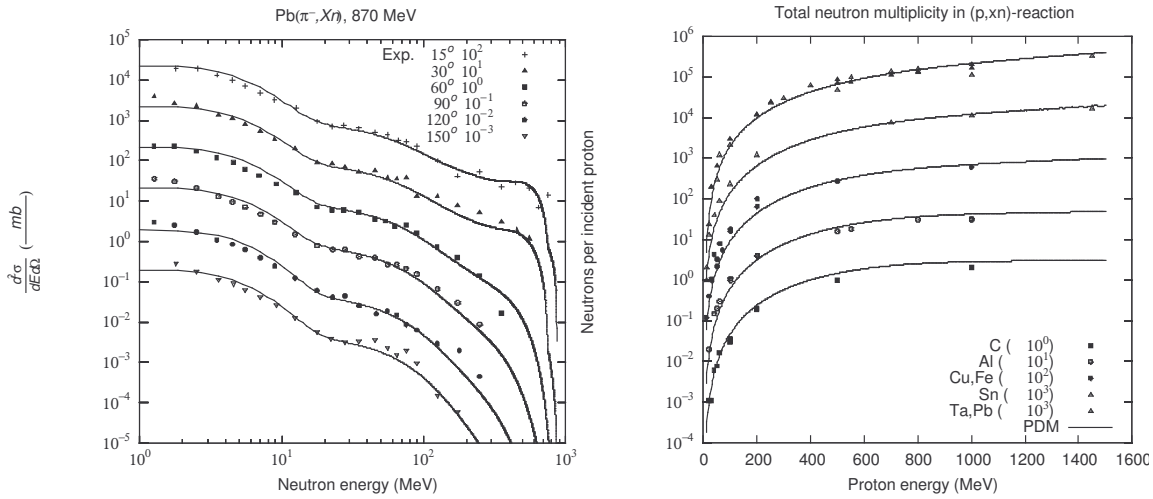

Figure 9. Comparison of neutron production cross section for Pb(π^-,Xn)-reaction at 870 MeV.

Figure 10. Comparison of total neutron multiplicity for proton-initiated reactions.

4.2. Thick target test calculations

Calorimetric measurements of the heat deposition inside thick cylindrical targets of different materials (Be, C, Al, Fe, Cu, W, Bi, Pb, W) described in Refs. [19,20]. The heat deposition calculations were carried out with LAHET 2.7 (Beard, 1995 [21]) and RTS&T codes. The results of theoretical and experimental data comparison for longitudinal distribution of energy deposition in cylindrical targets (d=20 cm, L=60 cm) of various materials under 1 GeV proton pencil-like beam irradiated are shown in Fig. 11.

Comparison of experimental neutron production spectra for 0.5, 1.0 and 1.2 GeV initial proton on Cu and W thick cylindrical targets (d=20 cm, L=60 cm) at 175^0 with calculated values by RTS&T code are shown on Fig. 12. The measurement was carried out using a booster in the IHEP (Protvino, Russian Federation). The energy of neutron produced in the target was measured by the Calorimetric-Time-Of-Flight (CTOF) method [22]. A Monte Carlo calculations were carried out by RTS&T code using the PDM hadronic generator. Comparison of total neutron yield (n/p) from cylindrical lead-target (d=20 cm, L=60 cm) under proton pencil-like beam irradiation as a function of incident energy is presented in Fig. 13

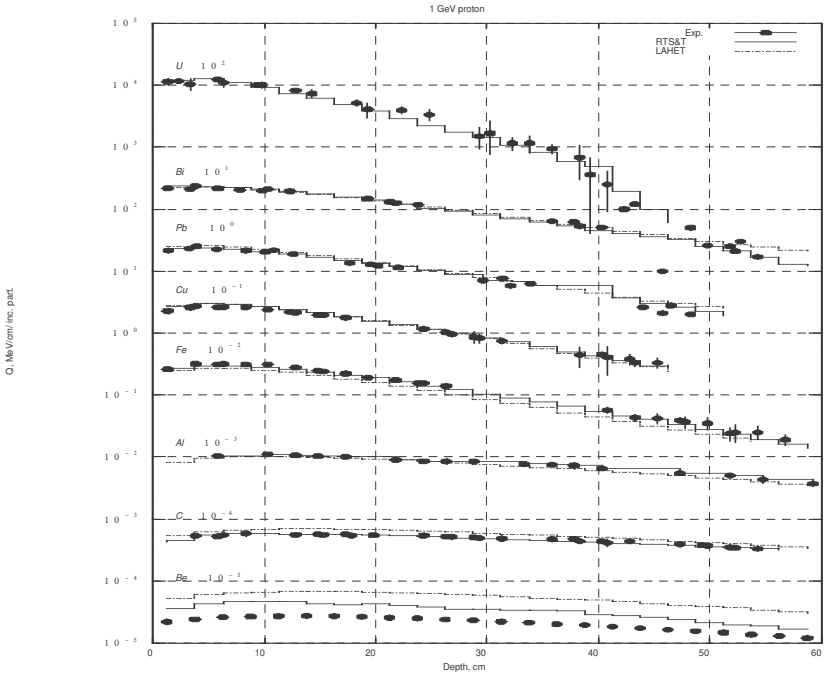

Figure 11. Comparison of heat deposition spectrum for (p,Xn)-reaction at 0.8 GeV.

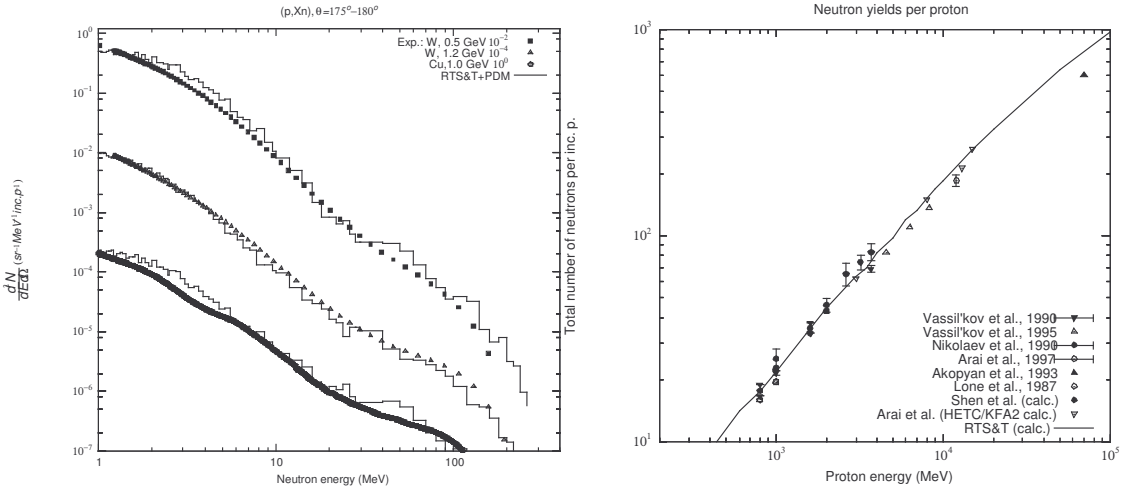

Figure 12. Comparison of neutron production spectrum for (p,Xn)-reaction at 175^o .

Figure 13. Comparison of total neutron yield from cylindric target under proton beam irradiation.

ASKNOWLEDGEMENTS

Authors wish to thank Prof. B.S. Sychev (Radiotechnical Institute of the Russian Academy of Sciences) for support and helpful discussions.

REFERENCES

1. A.I. Blokhin, I.I. Degtyarev et al., *Proc. of the SARE-3 Workshop*, KEK, 1997.
2. Y.K. Gambhir, S.H. Patil, *Z.Phys.* A321 (1985) 161.
3. V.V. Uzhinskii, S.Yu. Shmakov, Sov. *J. Nucl. Phys.* 57 No. 8, pp.1532-1533.
4. P. Moller et al., *NM 87545*, *CA 94720* (1995).
5. K.K. Gudima et al., *Nucl. Phys.* A401 p. 329 (1983).
6. B.S. Sychev, *Preprint of Radiotechnical Institute of the USSR Academy of Sciences*, No. 799 (1979).
7. B.S. Sychev, *Cross Sections of High-Energy Hadron Interactions with Atomic Nucl*ei, Radiotechnical Institute of the USSR Academy of Sciences, Moscow, 1999.
8. C. Kalbach, *Phys. Rev.* C 37 p. 2350 (1988).
9. C. Kalbach, *Phys. Rev.* C 41 (4) p.1656 (1990).
10. N.V. Mokhov et al., *IHEP Report 87-59*, Serpukhov (1987).
11. J. Ranft, *Phys. Rev.* D 51 p.64 (1995).
12. H. Pi, Fritiof 7.02, *Comp. Phys. Comm. Lib.*
13. V.V. Uzhinskii, *JINR Preprint* E2-96-192, Dubna (1996).
14. K. Werner, *Phys. Rep.* 232 p.87 (1993).
15. P. Cloth et al., *Proc. of a specialists' meeting Issy-Les-Moulineaux*, 1994, OECD 1994.
16. X. Ledoux et al., *Phys. Rev. Lett*. 82 (22) pp.4412-4415 (1999).
17. Y. Iwamoto et al., *J. of Nucl. Sci. and Tech.* Vol. 38, No. 6 pp.363-369 (2001).
18. S. Meigo et al., *Proc. of the 1999 Symposium on Nuclear Data*, INDC(JPN)-185/U.
19. V.I. Belyakov-Bodin et al., *Nucl. Instr. Meth*. A 295 p.140 (1990).
20. V.I. Belyakov-Bodin et al., *Nucl. Instr. Meth.* A 373 p.3 (1996).
21. C. Beard and V.I. Belyakov-Bodin, *Nucl. Sci. Eng*. 119 pp.87-96 (1995).
22. V.I. Belyakov-Bodin, I.I. Degtyarev et al., *Nucl. Instr. Met*h. A 465 pp.346-353 (2001).